Energy 107 (2016) 388–395

Contents lists available at ScienceDirect

Energy

journal homepage: www.elsevier.com/locate/energy

# Performance analysis of a dual loop thermally regenerative electrochemical cycle for waste heat recovery

Rui Long*, Baode Li, Zhichun Liu, Wei Liu*

*School of Energy and Power Engineering, Huazhong University of Science and Technology, Wuhan 430074, China*

ARTICLE INFO

*Article history:*
Received 15 May 2015
Received in revised form
4 March 2016
Accepted 12 April 2016
Available online 3 May 2016

*Keywords:*
Maximum power output
Finite time thermodynamics
Electrical efficiency
Thermally regenerative electrochemical cycle (TREC)
Dual loop thermally regenerative electrochemical cycle (DLTREC)

ABSTRACT

A DLTREC (dual loop thermally regenerative electrochemical cycle) system consisting of two hot electrochemical cells and a cold one is proposed for harvesting waste heat in a more efficient manner. With the maximum power output as the objective function, an optimal analysis of the DLTREC system based on a GA (genetic algorithm) method was conducted for different inlet temperatures of the heat source. For comparison, an optimization analysis of conventional TREC (thermally regenerative electrochemical cycle) systems was also conducted under equivalent criterion. The maximum output, the corresponding electrical and exergy efficiencies, and exergy destruction of the two energy harvesting systems were analyzed and compared. Results revealed that the DLTREC system can increase the power output and decrease the irreversibility. For the prescribed heat source inlet temperature of 393.15 K, the maximum power output of the DLTREC system was 50.11% larger than that of the conventional TREC system and the electrical efficiency was improved by 13.31%. The exergy efficiency of the DLTREC system was 19.41% larger than that of a conventional TREC system.



## 1. Introduction

In the past few decades, harvesting low-grade waste heat has received increasing attention. Many practical methods have been adopted for this objective. Thermodynamic cycles converting low grade thermal energy into electricity, such as the ORC (organic Rankine cycle), Kalina cycle, supercritical $CO_2$ cycle, and heat pipe technology have been extensively investigated for waste heat recovery and have been implemented for the recovery of low-grade thermal energy from various sources, including solar energy, exhaust gas from internal combustion engines, and geothermal sources [1–5]. Recently, electrochemical heat engines have been attracting more and more attention. In these engines, electrochemical reactions take place at different temperatures, resulting in electricity being generated from the energy difference between those two processes.

Generally, a single cycle is not able to efficiently recover the low-grade waste heat in a practical manner. Therefore, dual or combined cycles have been proposed for optimum recapturing utilization of waste heat. Meinel et al. [6] developed a two-stage ORC with internal heat recovery, in which the thermal efficiency was improved by 2.64%. Wang et al. [7] developed a novel system combining a dual loop ORC with a gasoline engine in which the thermal efficiency was increased by 3–6%. Shi et al. [8] researched a combined system, which consists of an ammonia–water mixture Rankine cycle and a LNG (liquefied natural gas) power generation cycle. Kong et al. [9] studied an energy system consisting of a gas turbine, an absorption chiller, and a heat recovery boiler. Li et al. [10] proposed a parallel double-evaporator ORC with the aim of decreasing system irreversibility and enhancing power output. Meng et al. [11] investigated the integration of a metal hydride system with a natural gas liquefier cycle plant for the cascade utilization of LNG (liquefied natural gas). Li et al. [12] investigated a new compound system that combined an ORC plant with a GHT (gathering heat tracing) station and an oil recovery system. Fu et al. [13] compared a Kalina cycle-based cascade utilization system to an existing ORC-based geothermal power system in an oilfield.

Additionally, thermoelectric materials and devices have been studied extensively in the past few decades [14–19]. Electrochemical heat engines offer an alternative method for the conversion of heat into electricity; one of which is the TREC (thermally regenerative electrochemical cycle). The TREC, which is a Stirling-like cycle, exhibits an efficiency of 40–50% of the Carnot limit for

* Corresponding authors. Tel.: +86 27 87542618; fax: +86 27 87540724.
*E-mail addresses:* R_Long@hust.edu.cn (R. Long), w_liu@hust.edu.cn (W. Liu).

http://dx.doi.org/10.1016/j.energy.2016.04.058
0360-5442/

high-temperature applications [20]. Recently, some literature has been concentrated on the application of applying TREC in harvesting low-grade thermal energy [21]. Based on finite time thermodynamics [22–25], the performance of the TREC has been systematically investigated [26]. Lee et al. [27] conducted an experiment on an electrochemical system for the efficient harvesting of low-grade heat energy. They found that the electrical efficiency reaches 5.7% when cycled between 10 and 60 °C. Yang et al. [21] proposed a charging-free TREC system, and an electrical efficiency of 2.0% was achieved for the TREC when operating between 20 and 60 °C. In addition, a membrane-free battery for the TREC was also been investigated resulting in an electrical efficiency of 3.5% when the battery was discharged at 15 °C and recharged at 55 °C [28]. Long et al. [29] adopted the TREC to harvest waste heat from the PEMFC (proton exchange membrane fuel cell), and found that the power output of the hybrid system is 6.85%–20.59% larger than that of the PEMFC subsystem, and the total electrical efficiency is improved by 2.74%–8.27%. In his later research, multi-objective optimization of a continuous TREC for waste heat recovery has also been conducted [30].

In this study, in order to recover waste heat more efficiently, a DLTREC (dual loop thermally regenerative electrochemical cycle) system is proposed. This system consists of two electrochemical cells exchanging heat with the heat source and one cell exchanging heat with the cold source, resulting in more heating being absorbed and more electricity being generated. With the maximum power output as the objective function, the DLTREC system was optimized under different heat source inlet temperatures. In addition, for comparison purposes, optimization of a conventional TREC system with the same objective function was also conducted. The maximum output, the corresponding electrical efficiency, exergy efficiency, and exergy destruction of the conventional and the DLTREC systems were analyzed and compared. The optimal open circuit voltages and current densities of the two systems were also analyzed.

## 2. Mathematical model of the DLTREC

The schematic diagram for the conventional TREC system is shown in Fig. 1. It contains two cells: a hot cell in contact with the heat source and a cold cell in contact with the cold source (for this study; cold water). Both the cells, in which the electrochemical reactions take place, also function as heat exchangers. The electrolyte solution was cycled through the two cells. A separator was placed inside the cell to conduct ions and prevent the reactants from spontaneously mixing as well as to prevent them from reacting without exchanging electrons through the external circuitry [31]. The TREC consists of four processes: heating, charging, cooling, and discharging. Because of the difference between the charging voltage and the discharging voltage, a net work equal to the difference between the charging and discharging energies is extracted.

In order to recapture the waste heat more efficiently, a DLTREC (dual loop thermally regenerative electrochemical cycle) system is proposed. As shown in Fig. 2, the thermal energy is first utilized by the upstream cell (HC1) and then by the downstream cell (HC2). To reduce the heat loss and to enhance the system efficiency, two regenerators were implemented. The electrolyte solution separates into two streams. One flows into HC2 and the other flows into HC1, where the electrochemical reaction takes place and the heat is absorbed. The electrolyte solution flows out of the cells, mixes in the mixer, and then goes into the CC (cold cell) where the electrochemical reaction takes place and heat is rejected. The schematic circuit diagrams of the conventional and DLTREC systems can be seen in Fig. 3. For the conventional TREC system, the current in the hot cell is equal to that in the cold one. As for the DLTREC system, the current in the cold cell is the sum of those in the two hot cells.

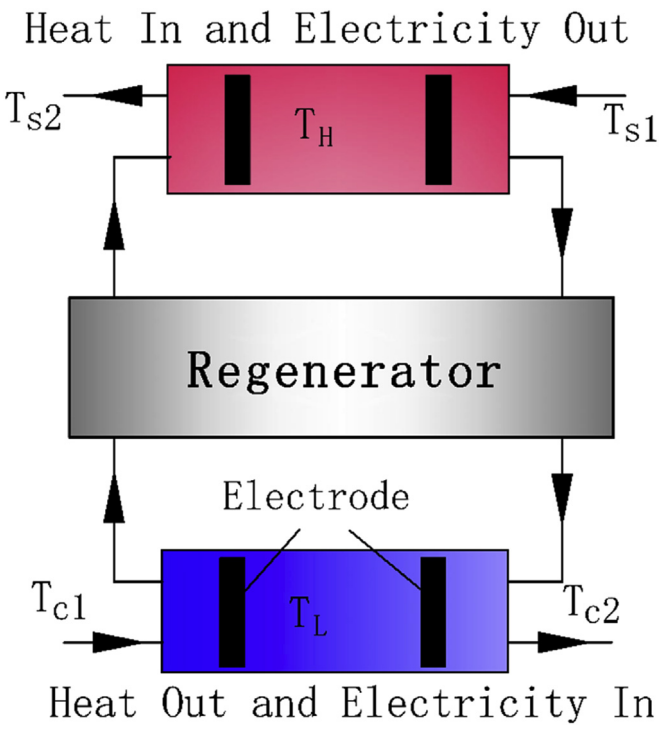


**Fig. 1.** Schematic of the conventional TREC system.

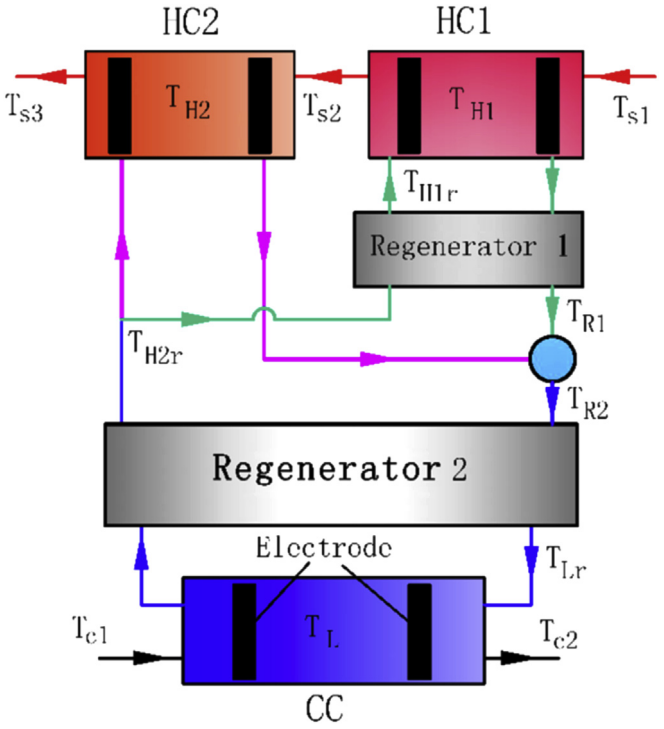


**Fig. 2.** Schematic of the proposed DLTREC system.

In an electrochemical reaction, an isothermal temperature coefficient may be defined when both electrodes are at the same temperature. For a full cell with an electrode reaction $\Sigma A \rightarrow \Sigma B$, the spontaneous reaction in the isothermal cell can be written

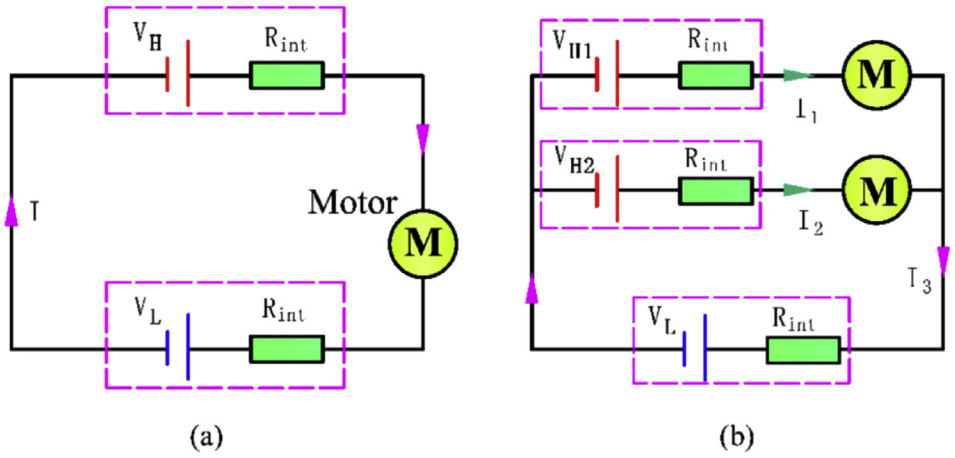


**Fig. 3.** Schematic circuit diagrams of the (a) conventional TREC system and the (b) DLTREC system.

as$\Sigma v_j C_j = 0$, where $C_j$ is the $j$th chemical involved and $v_j$ is its stoichiometric number. The isothermal coefficient for the full cell can be defined as [32].

$$\alpha_c = \left(\frac{\partial V_{oc}}{\partial T}\right)_{iso,T} = \frac{\Sigma v_j s_j}{nF} = \frac{\Delta \dot{s}}{nF} \tag{1}$$

where $V_{oc}$ is the open circuit voltage of the full cell in the isothermal condition. $s_j$ is the partial molar entropy of the $j$th chemical involved, $n$ is the number of moles of electrons passed per $v_j$ mole of $C_j$ reacted, and $F$ is the Faraday constant.

For HC1, from Eq. (1), the open circuit voltage is given by$V_{H1} = \alpha_c T_{H1}$. The reversible heat absorbed can be thus be calculated as

$$\dot{Q}_{H1} = T_{H1}\Delta \dot{S}_{H1} = \alpha_c \dot{n}_{e1} T_{H1} F \tag{2}$$

where $\dot{n}_{e1} = I_1/F$ is the molar flow rate of the reactant ion, $I_1 = i_1 A$ is the current, $i_1$ is the current density, and $A$ is the active surface. $\Delta \dot{S}_{H1}$ is the reversible entropy change in HC1.

The heat loss due to the resistance is

$$\dot{Q}_{loss1} = I_1^2 R_{int} \tag{3}$$

The heat loss originating from imperfect regeneration is

$$\Delta \dot{Q}_{Re1} = c_p \dot{n}_{es1}(1 - \eta_{re1})(T_{\mathrm{H1}} - T_{\mathrm{H2r}}) \tag{4}$$

where

$$T_{\mathrm{H2r}} = T_{\mathrm{L}} + \eta_{\mathrm{re2}}(T_{\mathrm{H2}} - T_{\mathrm{L}}) \tag{5}$$

and where $\eta_{\mathrm{re1}}$ and $\eta_{\mathrm{re2}}$ are the regenerative efficiency of the regenerators. $\dot{n}_{es1} = \dot{n}_{e1}/\varphi$ is the molar flow rate of the electrolyte solution in HC1. $\varphi$ is the molar percentage of the reactant in the electrolyte solution.

Taking into consideration the heat generated by the resistance, the total heat absorbed by HC1 is thus given by

$$\dot{Q}_{S1} = \dot{Q}_{H1} + \Delta \dot{Q}_{Re1} - \dot{Q}_{loss1} \tag{6}$$

Similarly, for HC2, the open circuit voltage is$V_{H2} = \alpha_c T_{H2}$ and the reversible heat absorbed is given by

$$\dot{Q}_{H2} = T_{H2}\Delta \dot{S}_{H2} = \alpha_c \dot{n}_{e2} T_{H2} F \tag{7}$$

where $\dot{n}_{e2} = I_2/F$ is the molar flow rate of the reactant ion in HC2. $I_2$ is the cell current.

The heat loss due to the resistance is therefore

$$\dot{Q}_{loss2} = I_2^2 R_{int} \tag{8}$$

The heat loss originating from imperfect regeneration is

$$\Delta \dot{Q}_{Re2} = c_p \dot{n}_{es2}(1 - \eta_{re2})(T_{\mathrm{H2}} - T_L) \tag{9}$$

where $\dot{n}_{es2} = \dot{n}_{e2}/\varphi$ is the molar flow rate of the electrolyte solution in HC2.

The total heat absorbed by HC2 is thus given by

$$\dot{Q}_{S2} = \dot{Q}_{H2} + \Delta \dot{Q}_{Re2} - \dot{Q}_{loss2} \tag{10}$$

Similarly, for the CC, the open circuit voltage is $V_L = \alpha_c T_L$, and the reversible heat released is given by

$$Q_L = T_L \Delta S_L = \alpha_c n_{e3} T_L F \tag{11}$$

where $\dot{n}_{e3}$ is the molar flow rate of the reactant ion. $I_3 = I_1 + I_2$ is the cell current.

The heat loss due to the resistance is therefore

$$\dot{Q}_{loss3} = I_3^2 R_{int} \tag{12}$$

The heat loss originating from imperfect regeneration is

$$\Delta \dot{Q}_{Re3} = c_p \dot{n}_{es3}(1 - \eta_{re1})(T_{\mathrm{H2}} - T_L) \tag{13}$$

where$\dot{n}_{es3}$ is the molar flow rate of the electrolyte solution in the CC.

The total heat rejected by the CC is thus given by

$$\dot{Q}_C = \dot{Q}_L + \dot{Q}_{loss3} + \Delta \dot{Q}_{Re3} \tag{14}$$

and the total heat absorbed from the heat source is

$$\dot{Q}_S = \dot{Q}_{S1} + \dot{Q}_{S2} \tag{15}$$

The power output is therefore given by

$$P = \dot{Q}_S - \dot{Q}_C = \alpha_c I_1 (T_{H1} - T_L) + \alpha_c I_2 (T_{H2} - T_L) - I_1^2 R_{int} - I_2^2 R_{int} - (I_1 + I_2)^2 R_{int} \quad (16)$$

and the electrical efficiency by

$$\eta_e = P/\dot{Q}_S \quad (17)$$

The exergy losses in each of the processes may also be calculated as follows.

Exergy destruction in HC1:

$$\dot{I}_{HC1} = T_0 \left[ \dot{n}_{es1} c_p \lg \frac{T_{H1}}{T_{H1r}} + \Delta S_{H1} - \frac{I_1^2 R_{int}}{T_{H1}} - \dot{m}_{hs}(s_{s1} - s_{s2}) \right]. \quad (18)$$

Exergy destruction in HC2:

$$\dot{I}_{HC2} = T_0 \left[ \dot{n}_{es2} c_p \lg \frac{T_{H2}}{T_{H2r}} + \Delta S_{H2} - \frac{I_2^2 R_{int}}{T_{H2}} - \dot{m}_{hs}(s_{s2} - s_{s3}) \right]. \quad (19)$$

Exergy destruction in the CC:

$$\dot{I}_{CC} = T_0 [\dot{m}_{cs}(s_{c2} - s_{c1}) - (\dot{n}_{es3} c_p \lg \frac{T_{Lr}}{T_L} + \Delta S_L + \frac{I_3^2 R_{int}}{T_L}] \quad (20)$$

Exergy destruction in Reg1:

$$\dot{I}_{Re1} = T_0 \dot{n}_{es1} c_p \left( \lg \frac{T_{H1r}}{T_{H2r}} - \lg \frac{T_{H1}}{T_{R1}} \right). \quad (21)$$

Exergy destruction in Reg2:

$$\dot{I}_{Re2} = T_0 c_p (\dot{n}_{es1} + \dot{n}_{es2}) \left( \lg \frac{T_{H2r}}{T_L} - \lg \frac{T_{R2}}{T_{Lr}} \right). \quad (22)$$

Exergy destruction in the mixer:

$$\dot{I}_{mix} = T_0 c_p \left( \dot{n}_{es2} \lg \frac{T_{R2}}{T_{H2}} - \dot{n}_{es1} \lg \frac{T_{R1}}{T_{R2}} \right). \quad (23)$$

It then follows that the total exergy loss is

$$\dot{I}_{Total} = \dot{I}_{HC1} + \dot{I}_{HC2} + \dot{I}_{CC} + \dot{I}_{Re1} + \dot{I}_{Re2} + \dot{I}_{mix} \quad (24)$$

and the exergy efficiency is defined as

$$\eta_{ex} = P/\Delta E_{hs}, \quad (25)$$

where the exergy decrease of the heat source is

$$\Delta E_{hs} = \dot{m}_{hs}[h_{s1} - h_{s3} - T_0(s_{s1} - s_{s3})]. \quad (26)$$

## 3. Results and discussion

GAs (Genetic algorithms) have been widely used in science and engineering as adaptive algorithms for solving practical problems and as computational models for natural evolutionary systems [20]. Performance optimizations based on genetic algorithms have been conducted by many researchers. In this work, with the maximum power output as the objective function, a GA method is employed to obtain optimal parameters for the DLTREC system for different heat source inlet temperatures, such as for the optimization of the working temperature of HC1 and HC2. For each case, the heat source inlet parameter is prescribed. The PPTDs (pinch point temperature differences) in the cells and the temperature of the cooling water are fixed and the regenerator efficiency for Reg1 and Reg2 are kept constant. The values of these input parameters for the calculation are listed in Table 1. In addition, the performance of a conventional TREC system under the same conditions, with maximum power output as the objective function, was also analyzed. The performance comparison is shown in Table 2.

Fig. 4 shows the curves of maximum power output of the conventional TREC system and the DLTREC system for different heat source inlet temperatures. The maximum power output of these two systems increases with increasing heat source inlet temperature. Their electrical efficiencies also exhibit a trend equivalent to that seen in Fig. 5. For the prescribed heat source inlet temperature of 393.15 K, the maximum power output of the DLTREC system was 50.11% greater than that of the conventional TREC system and the electrical efficiency improved by 13.31%, as shown in Table 2. Fig. 6 shows the exergy efficiency of the conventional TREC system as well as the DLTREC system under optimal conditions for different heat source inlet temperatures. The exergy efficiency of the DLTREC system increases with increasing inlet temperature. However, the energy efficiency of the conventional TREC system begins to increase with increasing inlet temperature, reaches a maximum value, and then decrease. When the inlet temperature of the heat source is 393.15 K, the exergy efficiency of the DLTREC system under optimal conditions was 19.41% greater than that of the conventional TREC system. Therefore, compared with the conventional TREC system, the DLTREC system can harvest waste heat more efficiently.

As shown in Fig. 7, under optimal conditions, the cell open circuit voltages of the hot cells of the conventional TREC system and the DLTREC system increase with increasing inlet temperature of the heat source. However, the cold cell open circuit voltages do not present obvious variations. This is because of the fact that the mass flow rate of the cooling water is too great, resulting in a constant operating temperature for the cold cell in both the conventional TREC system and the DLTREC system. The hot cell open circuit voltage of the conventional TREC system is slightly greater than that of HC1, but it is much greater than that of HC2. Fig. 8 illustrates the cell current densities of the conventional TREC system and the DLTREC system under optimal conditions for different heat source inlet temperatures. All the current densities increase with increasing inlet temperature of the heat source. In the cold cell, the current density of the DLTREC system was much larger than that of the conventional TREC system. Therefore, the heat loss due to the resistance was much greater.

The exergy destruction of the conventional TREC system and the DLTREC system under optimal conditions for given heat source inlet temperatures is shown in Fig. 9. Exergy destruction for each component increases with rising inlet temperatures. For both

**Table 1**
Prescribed parameters of the DLTREC system.

| Parameters | Notation | Value |
|---|---|---|
| Isothermal temperature coefficient [V/K] | $\alpha_c$ | $1.19 \times 10^{-3}$ |
| Heat source inlet temperature [K] | $T_{hs,in}$ | 323.15–393.15 |
| Mass flow rate of heat source [kg/s] | $\dot{m}_{hs}$ | 1 |
| Inlet temperature of cooling water [K] | $T_{cs,in}$ | 293.15 |
| Mass flow rate of cooling water [kg/s] | $\dot{m}_{cs}$ | 5 |
| PPTD in the hot cell [K] | $\Delta T_{PPTD,HC}$ | 4 |
| PPTD in the cold cell [K] | $\Delta T_{PPTD,CC}$ | 4 |
| Regenerative efficiency of Reg1 | $\eta_{re1}$ | 0.7 |
| Regenerative efficiency of Reg2 | $\eta_{re2}$ | 0.7 |

**Table 2**
Performance improvement of DLTREC compared with conventional TREC.

| Heat source inlet temperature | Performance improvement of DLTREC compared with conventional TREC | | |
|---|---|---|---|
| | $P$ | $\eta_{ex}$ | $\eta_{th}$ |
| 333.15 K | 56.20% | 5.46% | 11.41% |
| 343.15 K | 55.11% | 7.37% | 13.52% |
| 353.15 K | 54.06% | 8.66% | 14.93% |
| 363.15 K | 53.00% | 9.70% | 15.99% |
| 373.15 K | 51.99% | 11.05% | 17.31% |
| 383.15 K | 51.05% | 12.09% | 18.31% |
| 393.15 K | 50.11% | 13.31% | 19.41% |

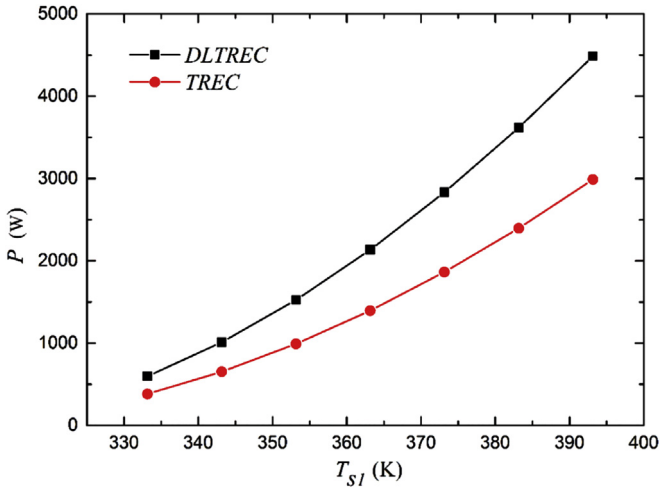


**Fig. 4.** Maximum power output of the conventional TREC system and the DLTREC system for different heat source inlet temperatures.

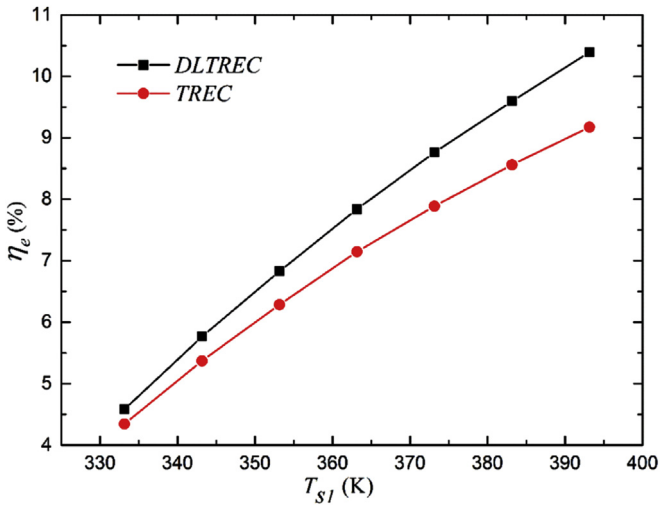


**Fig. 5.** Electrical efficiency of the conventional TREC system and the DLTREC system under optimal conditions for different heat source inlet temperatures.

systems, at lower inlet temperatures, the exergy destruction of the cold cell contributed the most, while at higher temperatures, that in the regenerators contributed the most. As shown in Fig. 10, for the DLTREC system at the prescribed heat source inlet temperature of 333.15 K, the exergy destruction in the cold cell was the largest of all, then followed by the two hot cells. When the inlet

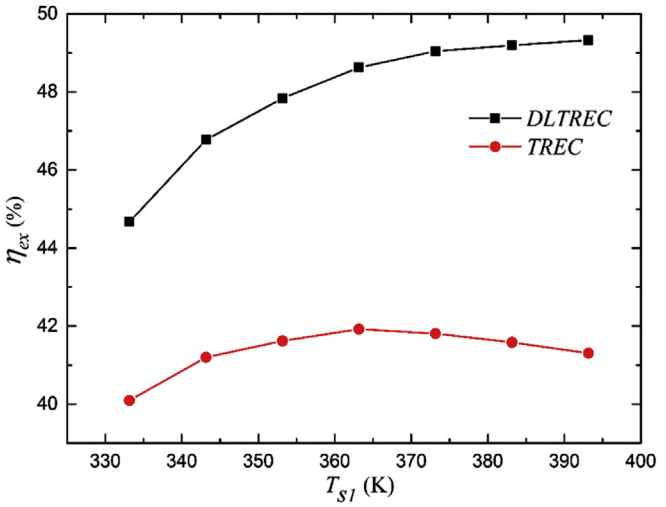


**Fig. 6.** Exergy efficiency of the conventional TREC system and the DLTREC system under optimal conditions for different heat source inlet temperatures.

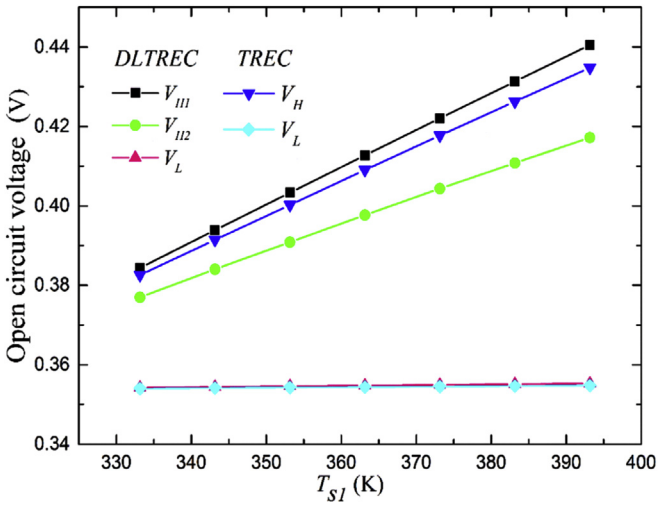


**Fig. 7.** Cell open circuit voltages of the conventional TREC system and the DLTREC system under optimal conditions for different heat source inlet temperatures.

temperature of the heat source was 393.15 K, the exergy destruction in the regenerator (Reg2) exceeded those in all other components, and took on the largest percentage of the total exergy destruction. However, the exergy destruction in the cold cell was only slightly less than that in Reg2. In addition, the mixer always contributed the least to the total exergy destruction of the DLTREC system.

It can be seen in Fig. 11, when the inlet temperature is less than 353.15 K, the total exergy destruction of the conventional TREC system is less than that of the DLTREC system. However when the inlet temperature is larger than 353.15 K, the exergy destruction of the conventional TREC system exceeds that of the DLTREC system with the difference becoming more and more prominent. At lower inlet temperatures, the increase in exergy destruction was mainly due to by the complexity of the DLTREC system. However, at higher inlet temperatures, the two hot cells (HC1 and HC2) can significantly decrease the exergy destruction in the heat absorption processes. In addition, the exergy destruction in the regenerators was reduced due to dual regeneration. The total exergy destruction was therefore improved.

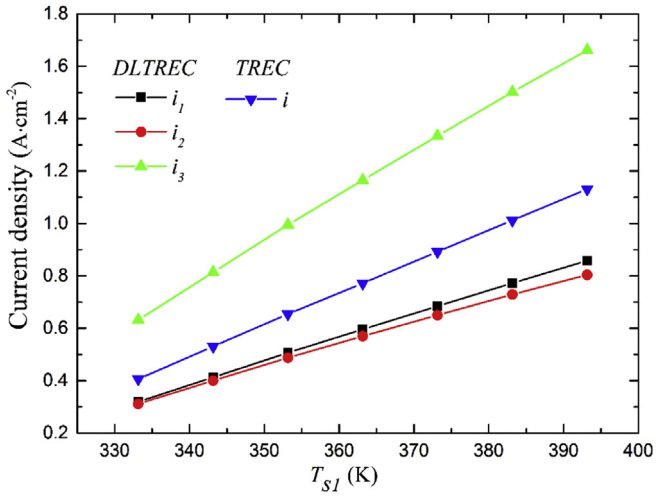


**Fig. 8.** Cell current densities of the conventional TREC system and the DLTREC system under optimal conditions for different heat source inlet temperatures.

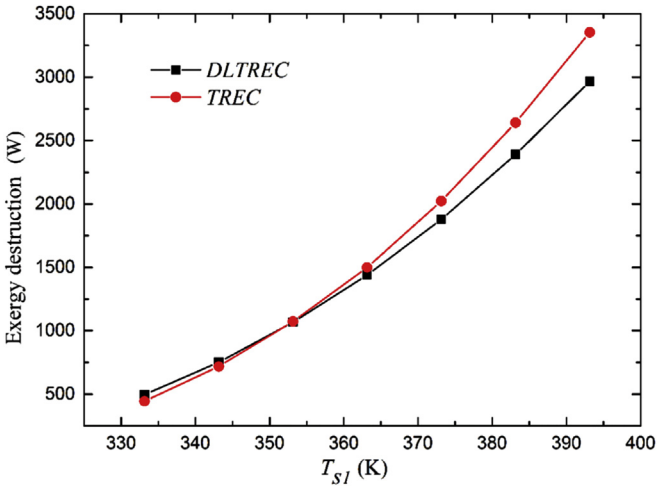


**Fig. 11.** Total exergy destruction of the conventional TREC system and the DLTREC system under optimal conditions at given heat source inlet temperatures.

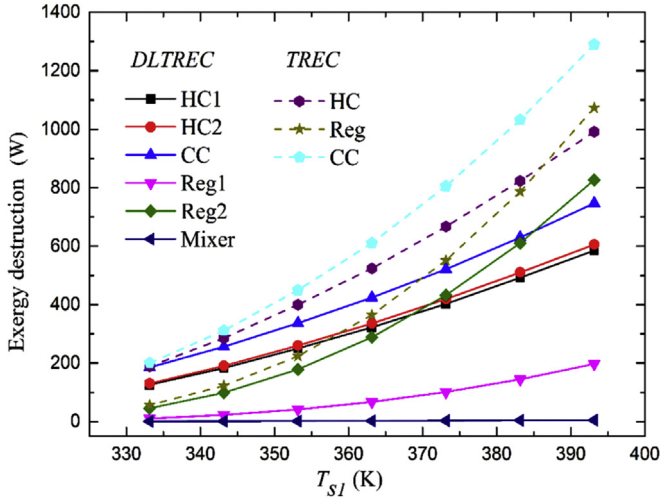


**Fig. 9.** Component exergy destruction of the conventional TREC system and the DLTREC system under optimal conditions at given heat source inlet temperatures.

## 4. Conclusions

In this paper, we discussed the study of a DLTREC system consisting of two hot electrochemical cells and a cold one. An optimization analysis of the DLTREC system based on genetic algorithm methods was conducted for different heat source inlet temperatures with the maximum power output as the objective function. The optimization analysis under the same criterion of a conventional TREC system was also compared. The maximum output, the corresponding electrical efficiency, exergy efficiency, and exergy destructions of the two energy harvesting systems were analyzed and compared. Results revealed that the power output as well as the electrical and exergy efficiencies of the DLTREC system all increase with increasing heat source inlet temperature. For the prescribed heat source inlet temperature of 393.15 K, the maximum power output of the DLTREC system was 50.11% greater than that of the conventional TREC system and the electrical efficiency improved by 13.31%. The exergy efficiency of the DLTREC system under optimal conditions was 19.41% greater than that of the conventional TREC system. This indicates that the proposed DLTREC system is capable of harvesting low-grade waste energy more efficiently.

Moreover, current thermoelectric efficiencies are usually lower than 0.5% when the heat source temperature is below 100 °C; while

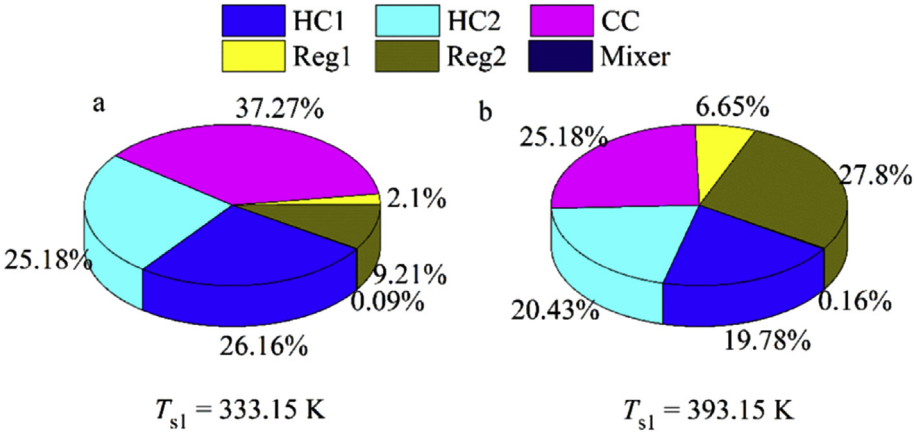


**Fig. 10.** Exergy destruction for different components under optimal conditions at heat source inlet temperatures of 333.15 K and 393.15 K for the DLTREC system.

the efficiency of the conventional TREC system can reach 3% [27]. And according to the aforementioned analysis, the performance of DLTREC is much better than that of the conventional one, which may offer a new way to efficiently recover low-grade waste heat. This DLTREC system could be applied to simultaneously recovery the wasted heat from the cooling water and exhausted gas in the gasoline or diesel engines, and to utilize solar energy [33]. But before it could be taken in application, the performance of the proposed DLTREC should be investigated experimentally, and the cost should been also considered. In addition, like the reverse TREC refrigeration system [34], refrigeration system based on reverse DLTREC could also been constructed for efficient and sufficient cooling.

## Acknowledgments

The work was supported by the National Key Basic Research Program of China (973 Program) (2013CB228302).

## Nomenclature

| | |
|---|---|
| $v$ | voltage [V] |
| $S$ | entropy [$W \cdot K^{-1}$] |
| $\alpha$ | isothermal coefficients [$V \cdot K^{-1}$] |
| $\dot{s}$ | partial molar entropy [$J \cdot mol^{-1} \cdot K^{-1}$] |
| $T$ | temperature [K] |
| $I$ | current [A] |
| $R_{int}$ | total internal resistance of cell [Ω] |
| $F$ | faraday constant [$C \cdot mol^{-1}$] |
| $G$ | Gibbs free energy [W] |
| $H$ | enthalpy[W] |
| $v$ | stoichiometric number |
| $n$ | number of moles of electrons |
| $\dot{n}_e$ | molar flow rate [$mol \cdot s^{-1}$] |
| $A$ | active surface area [$cm^2$] |
| $i$ | current density [$A \cdot cm^{-2}$] |
| $C_p$ | specific heat [$kJ \cdot mol^{-1} \cdot K^{-1}$] |
| $\dot{m}$ | flow rate [$kg \cdot s^{-1}$] |
| $T_0$ | ambient temperature [K] |
| $\dot{Q}$ | heat rate [W] |
| $\Delta\dot{Q}_{Re}$ | regenerative heat loss [W] |
| $\Delta\dot{Q}_{loss}$ | resistance heat loss [W] |
| $P$ | power output [W] |
| $\dot{I}$ | exergy destruction [W] |

*Subscripts and superscripts*

| | |
|---|---|
| c | cell |
| oc | open circuit |
| j | $j^{th}$ chemical involved |
| H | hot reservoir side |
| L | cold reservoir side |
| Re | regenerative |
| es | electrolyte solution |
| in | inlet |
| out | outlet |
| s, hs | heat source |
| c, cs | cooling source |
| H1,H1r,H2,H2r,R1,R2,Lr | state points |

*Greek symbols*

| | |
|---|---|
| $\eta_{re}$ | regenerative efficiency |
| $\eta_{ex}$ | electrical efficiency |
| $\varphi$ | molar percentage of the reactant |

*Acronyms*

| | |
|---|---|
| PPTD | pinch point temperature difference |
| TREC | thermally regenerative electrochemical cycle |
| DLTREC | dual loop thermally regenerative electrochemical cycle |
| HC1,HC2 | hot cell |
| CC | cold cell |

## References

[1] Wang R, Yu X, Ge T, Li T. The present and future of residential refrigeration, power generation and energy storage. Appl Therm Eng 2013;53(2):256–70.
[2] Tchanche BF, Lambrinos G, Frangoudakis A, Papadakis G. Low-grade heat conversion into power using organic Rankine cycles–a review of various applications. Renew Sustain Energy Rev 2011;15(8):3963–79.
[3] Franco A, Vaccaro M. On the use of heat pipe principle for the exploitation of medium–low temperature geothermal resources. Appl Therm Eng 2013;59(1–2):189–99.
[4] Long R, Bao YJ, Huang XM, Liu W. Exergy analysis and working fluid selection of organic Rankine cycle for low grade waste heat recovery. Energy 2014;73(0):475–83.
[5] Sprouse III C, Depcik C. Review of organic Rankine cycles for internal combustion engine exhaust waste heat recovery. Appl Therm Eng 2013;51(1):711–22.
[6] Meinel D, Wieland C, Spliethoff H. Effect and comparison of different working fluids on a two-stage organic rankine cycle (ORC) concept. Appl Therm Eng 2014;63(1):246–53.
[7] Wang E, Zhang H, Zhao Y, Fan B, Wu Y, Mu Q. Performance analysis of a novel system combining a dual loop organic Rankine cycle (ORC) with a gasoline engine. Energy 2012;43(1):385–95.
[8] Shi X, Che D. A combined power cycle utilizing low-temperature waste heat and LNG cold energy. Energy Convers Manag 2009;50(3):567–75.
[9] Kong X, Wang R, Huang X. Energy optimization model for a CCHP system with available gas turbines. Appl Therm Eng 2005;25(2):377–91.
[10] Li T, Zhu J, Hu K, Kang Z, Zhang W. Implementation of PDORC (parallel double-evaporator organic Rankine cycle) to enhance power output in oilfield. Energy 2014;68:680–7.
[11] Meng X, Bai F, Yang F, Bao Z, Zhang Z. Study of integrated metal hydrides heat pump and cascade utilization of liquefied natural gas cold energy recovery system. Int J Hydrogen Energy 2010;35(13):7236–45.
[12] Li T, Zhu J, Zhang W. Cascade utilization of low temperature geothermal water in oilfield combined power generation, gathering heat tracing and oil recovery. Appl Therm Eng 2012;40:27–35.
[13] Fu W, Zhu J, Li T, Zhang W, Li J. Comparison of a Kalina cycle based cascade utilization system with an existing organic Rankine cycle based geothermal power system in an oilfield. Appl Therm Eng 2013;58(1–2):224–33.
[14] Rosi F. Thermoelectricity and thermoelectric power generation. Solid-State Electron 1968;11(9):833–68.
[15] Bell LE. Cooling, heating, generating power, and recovering waste heat with thermoelectric systems. Science 2008;321(5895):1457–61.
[16] DiSalvo FJ. Thermoelectric cooling and power generation. Science 1999;285(5428):703–6.
[17] Gould C, Shammas N, Grainger S, Taylor I. A comprehensive review of thermoelectric technology, micro-electrical and power generation properties. 2008.
[18] Tritt TM, Subramanian M. Thermoelectric materials, phenomena, and applications: a bird's eye view. MRS Bull 2006;31(03):188–98.
[19] Chen G, Dresselhaus M, Dresselhaus G, Fleurial J-P, Caillat T. Recent developments in thermoelectric materials. Int Mater Rev 2003;48(1):45–66.
[20] Quickenden T, Mua Y. A review of power generation in aqueous thermogalvanic cells. J Electrochem Soc 1995;142(11):3985–94.
[21] Yang Y, Lee SW, Ghasemi H, Loomis J, Li X, Kraemer D, et al. Charging-free electrochemical system for harvesting low-grade thermal energy. Proc Natl Acad Sci 2014;111(48):17011–6.
[22] Açıkkalp E. Exergetic sustainability evaluation of irreversible Carnot refrigerator. Phys A Stat Mech Appl 2015;436:311–20.
[23] Açıkkalp E, Yamık H. Modeling and optimization of maximum available work for irreversible gas power cycles with temperature dependent specific heat. J Non-Equilibrium Thermodyn 2015;40(1):25–39.
[24] Curzon FL, Ahlborn B. Efficiency of a Carnot engine at maximum power output. Am J Phys 1975;43(1):22.
[25] Wu C. Recent advances in finite-time thermodynamics. Nova Publishers; 1999.
[26] Long R, Li B, Liu Z, Liu W. Performance analysis of a thermally regenerative electrochemical cycle for harvesting waste heat. Energy 2015;87:463–9.
[27] Lee SW, Yang Y, Lee H-W, Ghasemi H, Kraemer D, Chen G, et al. An electrochemical system for efficiently harvesting low-grade heat energy. Nat Commun 2014;5:3942.
[28] Yang Y, Loomis J, Ghasemi H, Lee SW, Wang YJ, Cui Y, et al. Membrane-free battery for harvesting low-grade thermal energy. Nano Lett 2014;14(11):6578–83.

[29] Long R, Li B, Liu Z, Liu W. A hybrid system using a regenerative electrochemical cycle to harvest waste heat from the proton exchange membrane fuel cell. Energy 2015;93:2079–86.
[30] Long R, Li B, Liu Z, Liu W. Multi-objective optimization of a continuous thermally regenerative electrochemical cycle for waste heat recovery. Energy 2015;93:1022–9.
[31] Gerlach DW, Newell T. An investigation of electrochemical methods for refrigeration. Air conditioning and refrigeration center. College of Engineering. University of Illinois at Urbana-Champaign; 2004.
[32] DeBethune A, Licht T, Swendeman N. The temperature coefficients of electrode potentials-the isothermal and thermal coefficients-the standard ionic entropy of electrochemical transport of the hydrogen ion. J Electrochem Soc 1959;106(7):616–25.
[33] Long R, Li B, Liu Z, Liu W. Performance analysis of a solar-powered solid state heat engine for electricity generation. Energy 2015;93:165–72.
[34] Long R, Li B, Liu Z, Liu W. Performance analysis of a solar-powered electrochemical refrigerator. Chem Eng J 2016;284:325–32.